# Validation of Temperature Compensation Techniques for Impact Damage Detection and Localization Using Ultrasonic Sparse Arrays

Michael Scheerer, Daniel Lager

# VALIDATION OF TEMPERATURE COMPENSATION TECHNIQUES FOR IMPACT DAMAGE DETECTION AND LOCALIZATION USING ULTRASONIC SPARSE ARRAYS

**Michael Scheerer[1], Daniel Lager[2]**

[1] *Aerospace & Advanced Composites GmbH, Viktor Kaplan Strasse 2, 2700 Wiener Neustadt*
[2] *Austrian Institute of Technology, Energy Department, Giefinggasse 2, 1210 Vienna*

michael.scheerer@aac-research.at

**ABSTRACT**

Within this paper the authors implemented and tested three different methods for temperature compensation – best baseline approach, signal interpolation and frequency shift – on thin monolithic composite plates and composite honeycomb panels together with the effectiveness of the different approaches for damage detection and localization under varying temperature conditions using sparse array configurations. The effectiveness of the different procedures have been compared and ranked. The best suited procedure – the frequency shift approach using the closest baseline measurement – was implemented in virtual beam forming algorithm used to visualize the ultrasonic image of the structure. Experiments have been conducted on an 800 x 800 mm² honeycomb panel instrumented with 4 piezo actuators and 8 piezo sensors. Different baseline measurements at various temperatures have been compared against measurement after the application of artificial damages using the best suited temperature compensation technique. It could be shown that temperature differences of several degrees between the baseline measurement and the measurement after damage introduction completely hides the appearance of the damage without using temperature compensation techniques. On the other hand all damages could be successfully detected and located when applying the proposed temperature compensation technique.

**KEYWORDS :** *Guided Ultrasonic Waves, Temperature Compensation, Composite Honeycomb Panels, Impact Damage*

## INTRODUCTION

Guided ultrasonic waves show high potential for online damage detection (Structural Health Monitoring) in different kind of structures as these waves can travel much larger distances compared to bulk waves. Therefore larger areas can be investigated with a limited number of permanently bonded actuators and sensors and no mechanical scanning is required. On the other hand the complex multimode, dispersive and especially in case of composite structures un-isotropic propagation characteristic of guided ultrasonic waves requires sophisticated signal processing procedures for a successful damage detection. One common procedure is to measure the ultrasonic response of an undamaged structure and subtract the results from the ultrasonic response after the occurrence of damage using exactly the same actuators and sensors. Beside the change of the ultrasonic signals caused by the presence of defects, changing environmental conditions such as temperature, humidity or applied stresses and strains lead to changes in the ultrasonic signals. Therefore good methods for the compensation of environmental effects are required. Different research groups around the world have proposed and tested methods for temperature compensation such as best baseline approach, signal stretching or combination of both methods [1, 2]. These methods have been investigated regarding their capability for improving impact damage detection and localization on honeycomb aircraft structures using guided ultrasonic waves in sparse array configuration.

## 1 INVESTIGATED COMPONENTS

The used components have been derived from a potential application – an Airbus A340 spoiler currently manufactured by FACC AG, where the impact critical regions are composed of the investigated honeycomb structures. In a first step a 400 x 400 mm² 0.75 mm thick face sheet of the honeycomb panel was instrumented with one piezo actuator surrounded by six piezo sensors on the top and bottom surface to measure the ultrasonic response at different frequencies, propagation directions and temperatures. The measurements were used to derive the dispersion curves for the two most important lamb wave modes – A0 and S0 as function of the propagation direction and temperature. In addition the raw data were fed in a post processing temperature compensation algorithm that allows the comparison of the different approaches. For the validation testing a flat honeycomb panel of 800 x 800 x 48 mm² has been used. The used materials and lay up for the face sheet and the honeycomb core have been taken from a spoiler of an Airbus A340 aircraft which is one possible application of Guided Wave SHM systems. The body is a CFRP sandwich construction with a honeycomb core. Two different core densities are used, the spoiler body being reinforced inside with a 48kg/m³ core and the center hinge fitting (CHF) with a 32kg/m³ core. The CFRP skins consist basically of 6 UD plies with an orientation of [-45/45/0/90/45/-45] on each side. Figure 1 shows the investigated components with the attached piezo sensors.


Figure 1: Investigated components with the attached piezo sensors (left side: face sheet, right side: honeycomb panel)

The material properties of the used face sheet material later used to calculate the group velocities of the ultrasonic waves are summarized in table 1.

Table 1: Material properties of face sheet and core

| $\rho$ [kg/m³] | $E_{\parallel}$ [GPa] | $E_{\perp}$ [GPa] | $G_{\perp\parallel}$ [GPa] | $G_{\perp\perp}$ [GPa] | $\nu_{\perp\parallel}$ | $\nu_{\perp\perp}$ |
|---|---|---|---|---|---|---|
| 1800 | 114.7 | 7.4 | 4.8 | 2.5 | 0.22 | 0.35 |

## 2 WAVE PROPAGATION IN THIN WALLED COMPOSITE STRUCTURES

The investigated components are made of honeycomb panels covered by thin face sheets on both sides. In order to detect defects in such structures by guided ultrasonic waves the characteristic of the propagating waves are very important. As the typical thicknesses of the face sheets, where the wave will mainly propagate are smaller than the wavelengths of these acoustic waves, these waves are confined and called therefore guided waves. These waves result out of the superposition of the bulk compression and shear waves and show the following characteristics:

- Different symmetric and asymmetric modes which number increase with the frequency are present in the structure
- Depending on the frequency all of these modes are more or less dispersive that means the wave velocity depend on the frequency
- When using un-isotropic composite materials the wave velocity depends on the direction of propagation
- The amplitude of the acoustic wave decrease with distance to the origin of the source due to natural wave spreading and material damping.
- Both wave spreading and damping depend on the wave mode, the frequency and in case of un-isotropic materials on the propagation direction.

## 2.1 Calculation of the group velocities

In a first step the wave velocity (phase and group velocity) of the face sheet were calculated in all necessary direction as function of the frequency using software DISPERSE. The results of wave velocity vs. frequency at different propagation directions for the face sheet are shown in Figure 2. The necessary input data are the elastic properties summarized in Table 1, the layup of [-45/45/0/90/45/-45] and the thickness of the face sheet of 0.75 mm.

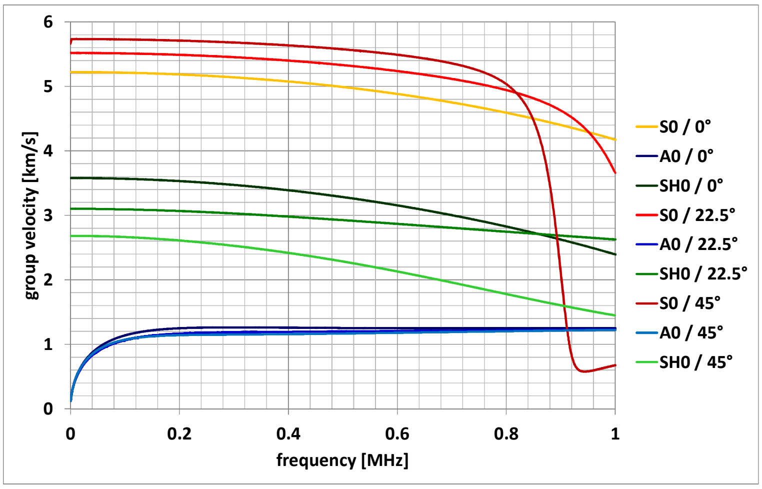


Figure 2: Dispersion relation of the 3 different lamb wave modes (A0, S0 and SH0) in face sheets up to a frequency of 1 MHz

It can be seen that all 3 existing modes (first symmetric S0, first asymmetric A0 and the first horizontal shear mode SH0) up to this frequency depend on the propagation direction and on the frequency. The A0 mode shows the highest dispersion (variation of the group velocity with the frequency) up to a frequency of around 100 kHz and the lowest sensitivity on the propagation direction. The S0 mode is the quickest mode with rather constant group velocity up to frequency of around 400 kHz. It shows a stronger dependence on the propagation direction where the direction of quickest propagation is in 45° and -45°. This effect is expected as the double amounts of fibers exist in these two directions compared to 0° or 90°. The SH0 mode shows a similar behaviour regarding the dependency on the propagation direction as the S0 mode.

## 2.2 Measurement of the wave propagation properties

After a first theoretical calculation of the wave velocities as function of the direction at room temperature a thin face sheet shown in figure 1 was instrumented with 8 piezo transducers. The actuator (8) was placed in the centre of the face sheet and 3 sensor pairs were placed at a distance of 150 mm from the actuator in directions 0° (sensor pair 1/2), 45° (sensor pair 3/4) and -45° (sensor pair 5/6), where one sensor was placed on the top and one on the bottom side of the face sheet to allow discrimination between symmetric and asymmetric guided wave modes. Measurement of the wave propagation have been performed at different center frequencies of the actuated burst signal between 20 kHz and 300 kHz in 10 kHz steps at different temperatures ranging from -40°C up to 80°C using the following system: data acquisition was done by two 4 channel acoustic emission cards (type PCI-DISP-4 from PAC) and the actuation was done by an arbitrary waveform generator card (type: ARB-1410 from PAC) which is actuated by Morlet wavelet of a voltage of 150 $V_{pp}$. The used transducers – actuators and sensors – were of type smart layer sensor from Acellant. All acquired signals are amplified with preamplifiers of type PAC WD with an amplification of 60 dB. Figure 3 show a typical measurement of the response of sensor 1 to a burst signal with a centre frequency of 60 kHz at different temperatures for the A0 mode.

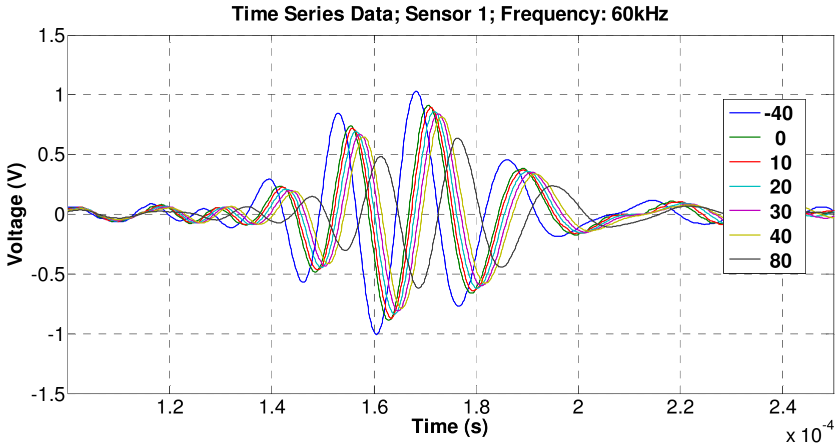


Figure 3: Typical measurement of the response of sensor 1 to a burst signal with a center frequency of 60 kHz at different temperatures (A0 mode)

It can be seen that the wave was shifted towards higher times with increasing temperature indicating a reduction of the group velocity with increasing temperature. In addition the amplitude decreases with increasing temperature caused by higher damping of the material and the adhesive with increasing temperature. The change in group velocity and the change in amplitude with temperature depend on the actuation frequency, the propagation direction and the wave mode. The measurement data were used as input for the evaluation of the efficiency of different temperature compensation methods described in the next chapter.

## 3 ALGORITHMS FOR TEMPERATURE COMPENSATION

Based on the basic observations, described before, different methods for temperature compensation were considered as following:

- Best baseline approach
- Signal interpolation approach
- Frequency shift approach (similar to signal stretch approach [1,2])

The simplest method to reduce temperature effects on damage detection capabilities is to subtract a baseline measurement which was performed at similar boundary conditions as the measurement performed after the appearance of damage – **best baseline**. Such method requires a lot of baseline measurements at different boundary conditions (in our investigations –temperatures).

In **"signal interpolation approach"** the signals of the individual sensors of baselines $B_i(T)$ are measured at pre-defined temperatures. During the measurement of the ultrasonic response of the structure after the potential occurrence of damage, the temperature has to be measured. For damage assessment in a first step the signals of the individual sensors of baseline measurements $B_i$ at two temperatures $T_{below}$ and $T_{above}$ around the temperature $T_{actual}$ of the actual measurement are linearly interpolated to calculate the signals of the individual sensors of a new baseline at the temperature of the actual measurement according to (1), where index "i" is the sample count.

$$B_i(T_{actual}) = \frac{[B_i(T_{above}) - B_i(T_{below})] \cdot [T_{acutal} - T_{below}]}{T_{above} - T_{below}} + B_i(T_{below}) \quad (1)$$

These calculated signals of the new virtual baseline measurement are subtracted from the actual measurement to derive the difference of both signals.

The **"frequency shift approach"** signals of the individual sensors of baseline $B_i(T_B)$ are measured at a pre-defined temperature "$T_B$". The measurement of the individual sensors after the potential occurrence of damage $D_i$ ($T_D$) can in generally be measured without the knowledge of the actual temperature $T_D$ although for better performance it is useful to know this temperature. The used frequency shift approach follows the logic of a general problem often referred as "Pitch Shifting" in music [3]. In a first step all signals that will be compared to each other like signals of a certain sensor before and after occurrence of damages or signals of a specific sensor measured at different temperatures were normalized according to (2).

$$B, D_{i,norm}(T_B) = \frac{B, D_i(T_B)}{\max_{0 \le i \le n}(B, D_i(T_B))} \quad (2)$$

Part of the normalized signal $D_{i,norm}$ in a pre-defined time window (expected arrival time of the A0 or S0 mode) was subjected to a shift of frequency using single-sideband modulation (SSB) by help of the Hilbert transform resulting in the analytic signal $D_{i,norm,ana}$ of $D_{i,norm.}$ The analytic signal was used to derive the frequency shifted signal – shift by $\omega_c$ – in time domain as shown in correlation (3).

$$D_{i,norm,shifted}(\omega_c) = Re\{e^{j\omega_c i T_s} D_{i,norm,ana}\} = \cos(\omega_c i T_s) \cdot D_{i,norm} + \sin(\omega_c i T_s) \cdot D_{i,norm,hilb} \quad (3)$$

where $D_{i,norm,ana}$ is the analytic signal, $\omega_c$ is the amount of frequency shift, $D_{i,norm}$ is the input signal and $D_{i,norm,hilb}$ is the Hilbert transform of the input signal, and $T_s$ is the sampling period.
Different frequency shifts have been applied to the signal $D_{i,norm}$ resulting in $D_{i,norm,shifted}$ ($\omega_c$). The standard deviations between $D_{i,norm,shifted}$ ($\omega_c$) and $B_{i,norm}$ as function of the frequency shift was determined. The minimum standard deviation between the two signal determines the optimum frequency shift for the best correlation of both signal and is selected as best suited frequency shift to obtain the new signal $D_{i,norm,shifted,min}$.

## 4 VALIDATION OF TEMPERATURE COMPENSATION ALGORITHMS

Both algorithms described before were implemented in a MATLAB® code and compared against each other on two different components – a thin face sheet and a honeycomb panel.

### 4.1 Validation on face sheet sample

The data measured on the face sheet described already in chapter 2.2 were used to evaluate the effectiveness of the developed algorithms. Therefore measurements performed at different frequencies and temperatures were compared against each other. The **signal interpolation approach** and **frequency shift approach** were used to correct data measured by a temperature different to the reference temperature and compare the corrected with the reference temperature as shown in figure 4 for the compensation of the A0 mode at 60 kHz.

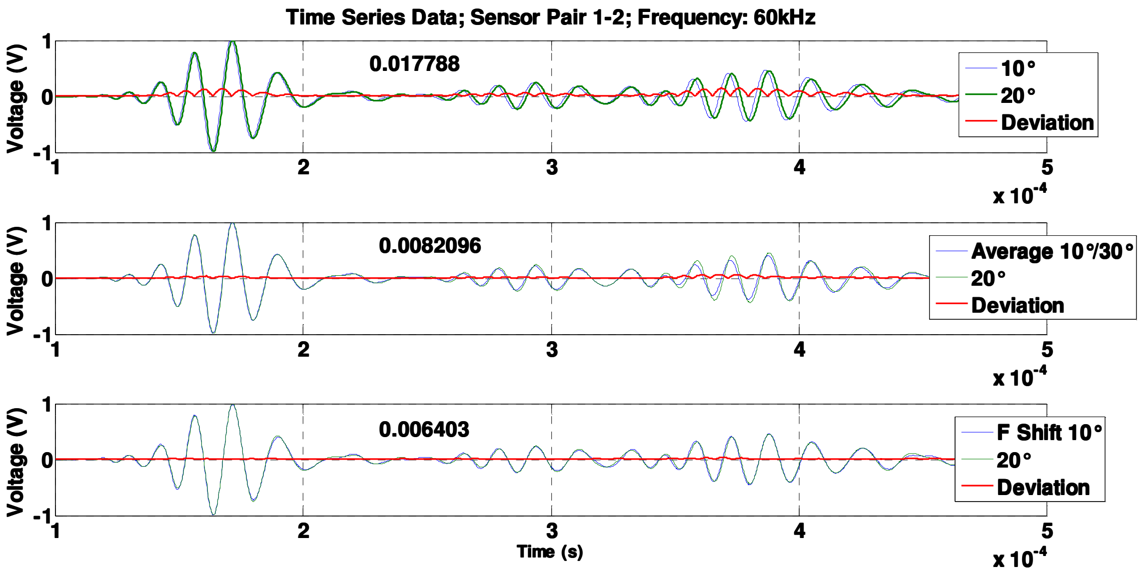


Figure 4: Effect of 2 different temperature compensation techniques for 60 kHz - compensation of A0 mode: top (comparison between baseline at 10°C and 20°C), middle: Reduction of residuum by interpolation, bottom: Reduction of residuum by frequency shift

Three measurements have been used at 10°C, 20°C and 30°C, where the 10°C and the 30°C measurement were averaged using the **signal interpolation approach** and the 10°C measurement was shifted towards the 20°C measurement using the **frequency shift approach** and compared to the 20°C measurement. The numbers in Figure 4 give the standard deviation between the compared curves. It can be seen that the smallest standard deviations have been obtained by the frequency shift approach. Similar results have been achieved for both wave modes A0 and S0 over the whole frequency range in all three propagation directions. A roughly linear behaviour has been observed between optimum frequency shift and the temperature difference between the compared measurements. Figure 4 shows the standard deviation in dB for both approaches as function of the frequency for the A0 mode and the optimum average frequency shift / temperature as function of the frequency and the mode for sensor pair 1-2.

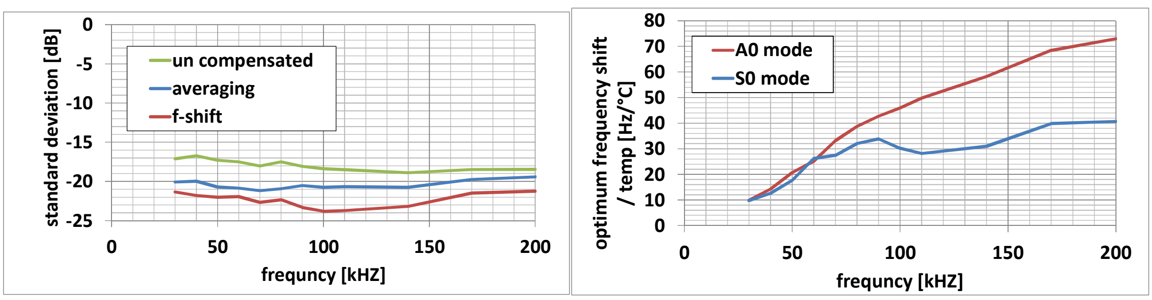


Figure 5: Left: Standard deviation in dB for both approaches as function of the frequency for the A0 mode Right: Optimum average frequency shift / temperature as function of the frequency and the mode for sensor pair 1-2

### 4.2 Validation on honeycomb panel using sparse arrays

In the used honeycomb panel shown in Fig. 1, totally 12 piezo transducer were placed along the boundaries. Four transducers placed at the edges were used as actuators and the remaining 8 were used to measure the ultrasonic waves. Following steps were used in the post processing algorithm allowing the imaging of the acoustic response of the structure. In a 1st step the raw data from all piezo sensors were filtered using an FIR (or respectively FFT) band pass filter to remove the noise and direct current content. In a 2nd step the filtered signals coming from two different measurements – baseline measurement and measurement after the introduction of the impact are compared to each other in order to compensate environmental effects by the **frequency shift approach**. The 3rd step is used to visualize the results by transferring the filtered and corrected transient signals from the time domain to the 2-dimensional space domain. Therefore a near-field beam forming algorithm was used described in more detail in [4, 5]. All mentioned steps described above were implemented in MATLAB® that allows an automated evaluation of the raw data collected by the individual piezo sensors.

In a first validation step the honeycomb panel was placed in a climate chamber and baseline measurements at different actuation frequencies and temperatures ranging from 0°C up to 50°C were performed. These measurements have been fed in the post processing algorithm described above to evaluate the residual signals between the individual measurements with and without application of the temperature compensation by the **frequency shift approach**. Figure 5 show the 2D colour coded residual distribution between three baseline measurements performed at 1.3 °C, 20.7°C and 29.2 °C without and with frequency shift for 40 kHz using the wave velocity of 785 m/s of the A0 mode for image reconstruction.

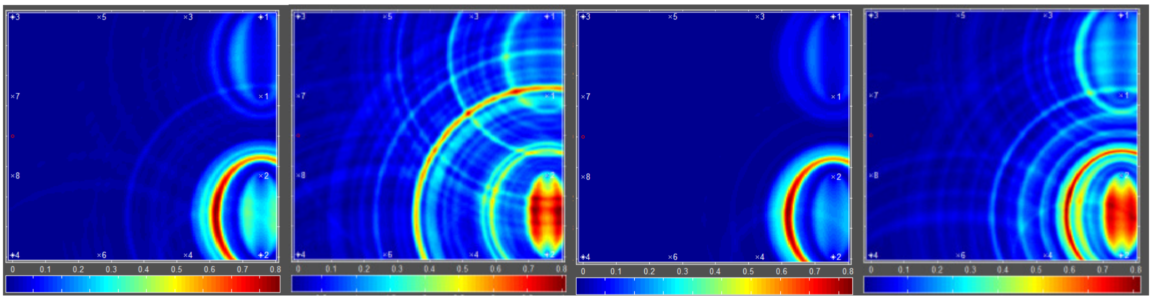

0 $9.5\cdot10^{-3}$ 0 $4\cdot10^{-4}$ 0 $4.6\cdot10^{-2}$ 0 $3\cdot10^{-3}$

Figure 6: 2D colour coded residual distribution between different baseline measurements at 40 kHz using the wave velocity of 850 m/s of the A0 mode for image reconstruction: between 20.7°C and 29.2 °C without (1) and with frequency shift (2) and between 1.3°C and 29.2 °C without (3) and with frequency shift (4).

The application of the frequency shift lead to reduction of the maximum residuum by a factor of 22 for the compensation between 20.7°C and 29.2 °C and by a factor of 15 between 1.3°C and 29.2 °C. In addition also the achievable maximum residuum increases with higher temperature difference between the individual measurements by roughly an order of magnitude if the temperature difference between the measurements is increased from 8.5°C to 27.9°C.

Finally impact damages with a damage size of around 900 mm² (incident energy of 44 J) have been introduced on the different positions of the panel. The measurements of the response after the introduction of the impacts have been compared to baseline measurements at different temperatures to assess the possibility for damage detection and localization with and without the frequency shift approach. Figure 5 shows the 2D colour coded images of the residual signals between a baseline measured at 20°C and the impact measured at 24°C without and with frequency shift for 40 kHz using the wave velocity of 785 m/s of the A0 mode for image reconstruction.

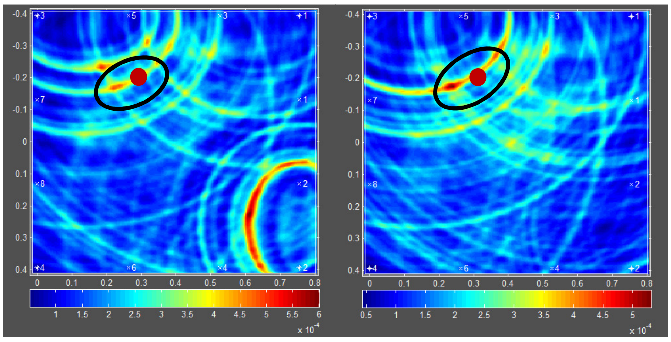

Figure 7: 2D colour coded images of the residual signals between the baseline measured at 20°C and the impact measured at 24°C without (left side) and with frequency shift (right side) for 40 kHz using the wave velocity of 785 m/s of the A0 mode for image reconstruction. The red circle indicates the impact position.

The application of the frequency shift lead to better determination of the impact position by a clear reduction of artefacts in the 2D images of the residual signals. It has to be noted that the application of the frequency shift algorithm in sparse array configuration and multimode wave propagation is limited to temperature differences to around 5°C in the investigated structures as only one mode can be compensated and the other mode still produces artefacts in the images.

## CONCLUSION

Within this paper the authors presented different approaches for temperature compensation which have been applied on composite face sheets and honeycomb panels. The following conclusions can be drawn:

- When comparing signal interpolation and frequency shift approach, the frequency shift approach allows better compensation of temperature induced effects.
- The optimum shift frequency depends on the wave propagation mode, the frequency and in case of the used un-isotropic face sheets the propagation direction.
- The application of the frequency shift approach on honeycomb panels subjected to baseline measurements at different temperatures lead to a reduction of the residuum distribution over the panel that depends on the used wave velocity for image reconstruction – A0 or S0 mode and the frequency.
- The application of the frequency shift approach lead to better identification and localization of impact damages as long as the temperatures used for the measurement of the baseline and the impact measurement to not differ by more than 5°C.

## REFERENCES

[1] T.Clarke, F.Simonetti, P.Cawley: “Guided wave health monitoring of complex structures by sparse array systems: Influence of temperature changes on performance”, Journal of Sound and Vibration 329 (2010) 2306–2322
[2] Anthony J. Croxford, Jochen Moll, Paul D. Wilcox, Jennifer E. Michaels: “Efficient temperature compensation strategies for guided wave structural health monitoring”, Ultrasonics 50 (2010) 517–528
[3] Habib Estephan, Scott Sawyer, Daniel Wanninger: “Real-Time Speech Pitch Shifting on an FPGA”, http://homepage.villanova.edu/scott.sawyer/fpga
[4] M. Scheerer, C. Bockenheimer, A. Dantele, Z. Djinovic, F. Graf, T. Natschläger, A. Peldszus, M. Reiterer, T. Sauter, R. Stössel: „ Development and testing of an ultrasonic phased array system based on piezo actuators and fiber optic sensors”, Proc. of the IWSHM 2011, Stanford, USA, 2011, pp. 447 - 454
[5] M.Scheerer, D. Lager, F. Göral: „Development and Testing of a Hybrid Active – Passive Acoustic SHM System for Impact Damage Detection in Honeycomb Aircraft Structures”, Proc. of the 19th ICCM, Montreal, Can, 2013, pp. 7154 - 7165